APS physics

CHORUS

This is the accepted manuscript made available via CHORUS. The article has been published as:

Anisotropic excitonic effects in the energy loss function of hexagonal boron nitride

S. Galambosi, L. Wirtz, J. A. Soininen, J. Serrano, A. Marini, K. Watanabe, T. Taniguchi, S. Huotari, A. Rubio, and K. Hämäläinen

Phys. Rev. B **83**, 081413 — Published 23 February 2011

DOI: 10.1103/PhysRevB.83.081413

Anisotropic excitonic effects in the energy loss function of hexagonal boron nitride

S. Galambosi,[1] L. Wirtz,[2] J. A. Soininen,[1] J. Serrano,[3] A. Marini,[4,5,6]
K. Watanabe,[7] T. Taniguchi,[7] S. Huotari,[8,1] A. Rubio,[6] and K. Hämäläinen[1]

[1]*Department of Physics, POB 64, FI-00014 University of Helsinki, Finland*
[2]*IEMN, CNRS UMR 8520, Dept. ISEN, B.P. 60069, 59652 Villeneuve d'Ascq, France*
[3]*ICREA–Departamento de Fisica Aplicada, Universitat Politecnica de Catalunya, EPSC, Av. Esteve Terradas 15, 08860 Castelldefels, Spain*
[4]*IKERBASQUE, Basque Foundation for Science, E-48011 Bilbao, Spain*
[5]*European Theoretical Spectroscopy Facility (ETSF) and Dipartimento di Fisica, Università di Roma "Tor Vergata", via della Ricerca Scientifica 1, 00133 Roma, Italy*
[6]*Nano-Bio Spectroscopy Group, ETSF Scientific Development Centre, Universidad del País Vasco, CFM-CSIC-UPV/EHU-MPC and DIPC, Av. Tolosa 72, E-20018 San Sebastián, Spain*
[7]*National Institute for Materials Science, 1-1 Namiki, Tsukuba, 305-0044, Japan*
[8]*European Synchrotron Radiation Facility, BP 220, F-38043 Grenoble cedex, France*

The anisotropy of the valence energy-loss function of hexagonal boron nitride (*h*BN) is shown to be largely enhanced by the highly inhomogeneous character of the excitonic states. The energy loss with momentum transfer parallel to the BN layers is dominated by strongly bound, quasi-2D, excitons. In contrast, excitations with momentum transfer perpendicular to the layers are influenced by weakly bound 3D excitons. This striking phenomenon is revealed by a combined study using high precision non-resonant inelastic x-ray scattering measurements supported by ab-initio calculations. The results are relevant in general to layered insulating systems.

NOT FOR CIRCULATION

Layered hexagonal boron nitride is the III-V counterpart of graphite, but due to the different electronegativities of boron and nitrogen, it has a large band gap. In recent work[1] it was shown that *h*BN exhibits the potential for lasing at high energies (5.8 eV) making it an attractive candidate for optoelectronic applications in the ultraviolet energy range. Despite the relatively simple crystal structure, *h*BN appears to be a challenge to both experiments and theory. On the experimental side, the challenge is the fabrication of high quality single crystals which has been achieved only recently[2]. On the theoretical side, it is well established that the band-structure of *h*BN displays an indirect gap[3,4] and the optical absorption spectrum is dominated by correlation effects leading to a strong Frenkel-type excitonic peak at 5.8 eV[4–6] in agreement with the experimental findings[1]. However, the origin of the fine structure of the absorption and luminescence spectra around this peak is still under debate[7–9]. Recent luminescence experiments point towards the role of defects[10,11] in agreement with the theoretical suggestion in ref. 7.

In this article, we study the dynamics (dispersion) of the valence excitations of *h*BN using non-resonant inelastic x-ray scattering (NRIXS). Compared to electron energy loss spectroscopy (EELS), NRIXS is better suited for studying the dispersion of low lying excitations also beyond the first Brillouin zone (1st BZ). This has been used numerous times in the past (see e.g.[12,13]) and gives new important information on the properties of excitations at sub-unit-cell length scales[14]. When studying longitudinal excitations one often finds non-parabolic dispersions[15] and periodicity for low energy plasmons[16,17].

We show detailed experimental results of the dispersion of various features and plasmons for the momentum transfer $\mathbf{q}$ in different crystallographic directions. The loss features show a strong directional dependence not only in the comparison in-plane/out-of-plane but also for the different directions within the plane. The origin of the different spectral features and their direction and momentum dependence are analyzed by *ab-initio* many-body perturbation theory calculations. Beyond the well-known anisotropy of the electronic band structure, we find suprisingly that also the electron-hole interaction has a strong anisotropy. Taking this anisotropy into account may be important in layered materials in general.

The sample was a colorless and transparent hexagonal single crystal *h*BN platelet about 700 μm wide and 70 μm thick[18]. The ΓA direction was found to be very nearly parallel to the normal of the platelet. We used single-crystal X-ray diffraction to verify that the sample exhibited an AB-type stacking, thus ruling out other stable or metastable stacking sequences[19,20].

The NRIXS spectra were measured on ID16 at the European Synchrotron Radiation Facility, Grenoble, France. The experiment was carried out using the eV-resolution spectrometer[21,22]. An energy resolution of 0.6 eV was determined from the FWHM of the quasi-elastic line. The measurements were performed using the inverse scan technique[23]. The momentum transfer resolution was $\Delta q/q \approx 0.17$ near the K point.

The valence bands and the lowest conduction bands of *h*BN can be understood as combinations of the σ and π states of the hexagonal boron nitride sheet. At low momentum transfer the low-energy-transfer structures of the loss function can be divided into transitions between states with same parity (σ-$\sigma*$, π-$\pi*$) when the momentum transfer is in the plane and different parity (π-$\sigma*$, σ-$\pi*$) for momentum transfer along the c-axis[24]. The strong anisotropy in the electronic response can also be seen in the difference for the dielectric constants ε_∞ par-

allel and perpendicular to the planes (4.40 and 2.53, respectively[4]). Theoretical NRIXS spectra have been calculated at the level of the random-phase approximation (RPA) starting with the Kohn-Sham DFT wavefunctions in the local-density approximation (LDA)[25]. The dielectric function is obtained through $\epsilon_{\mathbf{G},\mathbf{G}'}(\tilde{\mathbf{q}},\omega) = 1 - v(\tilde{\mathbf{q}}+\mathbf{G})\chi^0_{\mathbf{G},\mathbf{G}'}(\tilde{\mathbf{q}},\omega)$, where $v(\tilde{\mathbf{q}}) = 4\pi/|\tilde{\mathbf{q}}|^2$ is the Coulomb potential in reciprocal space and $\chi^0_{\mathbf{G},\mathbf{G}'}(\tilde{\mathbf{q}},\omega)$ is the independent particle polarizability which is obtained from a sum over transitions from occupied to unoccupied bands[26]. $\mathbf{G},\mathbf{G}'$ denote reciprocal lattice vectors, and $\tilde{\mathbf{q}}$ is restricted to the 1st BZ.

The loss function $\sigma(\mathbf{q},\omega)$, which is the experimentally probed quantity is obtained from the inverse of the dielectric matrix $\sigma(\tilde{\mathbf{q}}+\mathbf{G},\omega) = -\mathrm{Im}(\epsilon^{-1}_{\mathbf{G},\mathbf{G}}(\tilde{\mathbf{q}},\omega))$, where $\mathbf{q} = \tilde{\mathbf{q}} + \mathbf{G}$. Crystal local-field effects are automatically included by taking into account the off-diagonal elements of $\epsilon_{\mathbf{G},\mathbf{G}'}$ in the matrix inversion[27,28]. In order to compare with the experimental loss function, we have used a broadening $\eta = 0.6$ eV. We have checked that the use of time dependent LDA does not give any substantial improvement.

The experimental and theoretical NRIXS spectra along three crystallographic directions for low values of q are depicted in Fig. 1. The experimental spectra were normalized to the same area as the calculated ones. Overall, the calculations reproduce the experimental spectra well. The *ab-initio* calculations match the experimental feature positions, their relative weights as well as the momentum transfer dependence. From the figure it is evident that the spectral features along the ΓA direction do not exhibit any significant dispersion. The high anisotropy of *h*BN is clearly reflected in the differences between the spectra in the hexagonal plane (ΓK, ΓM) and the spectrum perpendicular to it (ΓA). For $q \lesssim 0.6$Å^{-1}, the spectra along ΓK and ΓM are nearly identical. However, as the value of q is increased an anisotropy also within the hexagonal plane is clearly observed. In the high-energy range this anisotropy shows up mainly as a different rate of relative spectral weight increase for the feature between 35 eV-40 eV. The in-plane anisotropy is most evident in the behavior of the π plasmon. Its energy disperses from 9 eV at small values of momentum transfer to about 12 eV when q is near the boundary of the 1st BZ. Along ΓM an additional peak around 8 eV develops for $q > 0.87$ Å^{-1} while in the ΓK direction only a weak shoulder is detected. The double-peak structure along ΓM is also visible in $\mathrm{Im}(\epsilon(\mathbf{q}))$. This indicates that the directional anisotropy can be interpreted in terms of interband transitions. Fig. 2 (a) shows the band structure of *h*BN. For $\mathbf{q} = \Gamma K$, the transitions that dominate the plasmon at 12 eV are the ones from the π band at A/H to the π^* band at H/A, respectively (red arrows). For $\mathbf{q} = \Gamma M$, the dominant transitions are the ones from the π band at A/L to the π^* band at L/A (blue arrows). The observed 8 eV transition at $\mathbf{q} = \Gamma M$ originates from a $\pi - \pi^*$ interband transition from L to a neighboring high symmetry point L'. This is marked by the vertical green arrow in Fig. 2 (a) even though it is not a vertical transition but one with with a momentum difference of $\mathbf{q} = \Gamma M$. At $\mathbf{q} = \Gamma K$ the plasmon peak around 8 eV is missing because the joint-density of states displays only a minor peak there.

In order to align with the low energy experimental features the ΓM and ΓK theoretical spectra have been blueshifted by 0.8 eV whereas for the ΓA spectra a blueshift of 1.5 eV was used. These shifts reflect the well-known fact that the DFT band-structure usually underestimates the transition energies between occupied and unoccupied bands. For *h*BN it was shown[3,4,7] that electron-electron correlation, calculated on the level of the GW-approximation, increases the transition energies by about 2 eV with respect to DFT-LDA calculations. At the same time, the attractive electron-hole interaction reduces the transition energy such that the difference between experimental and theoretical NRIXS spectra is less than 2 eV. We note that the GW-correction alone cannot explain the observed anisotropic shift since π and σ bands are renormalized in the same way. Therefore the experimental NRIXS data cannot be explained with single particle theories and the explicit inclusion of electron-hole interaction is necessary.

In order to check if the combined effect of electron-electron and electron-hole interaction does indeed explain the (anisotropic) shift of the RPA-spectra, we carried out parameter-free calculations at selected momentum transfers including excitonic effects on the level of the Bethe-Salpeter Equation (BSE)[29]. We used the approach of Refs. 15,30 and converged all the relevant parameters[31]. To approximate the quasi-particle band energies of Ref. 7, we used a "scissor" of 1.92 eV to shift the LDA conduction bands energies and a small stretch of 5% was applied to the valence bands. As shown in Fig. 3 the BSE results agree well with the experimental and the blueshifted RPA spectra. The slight differences between the two calculations seem to originate mainly from different weights of various spectral features. Also, it should be noted, that (except for the energy shift) no extra features seem to arise in the BSE results in comparison with the RPA calculations. This confirms that the RPA successfully describes long–range excitations even in strongly anisotropic and layered materials like *h*BN, with the BSE leading only to minor corrections. Electron-hole effects can alter extended excitations only when the attraction is very strong, like in a wide-gap insulators such as LiF[29].

Thus we find that due to the the layered structure of *h*BN not only the electronic structure but importantly also the electron-hole interaction is highly anisotropic. This is elaborated in Fig. 2 b) and c) where we show the excitonic "wave functions" for the lowest visible excitations in the optical absorption spectrum. For q parallel to the planes ($q_\parallel$), electron and hole are localized within one plane forming a strongly bound quasi-two dimensional compound[4,7]. For q perpendicular ($q_\perp$), electron and hole are localized on different layers and form a more weakly bound three-dimensional compound. This

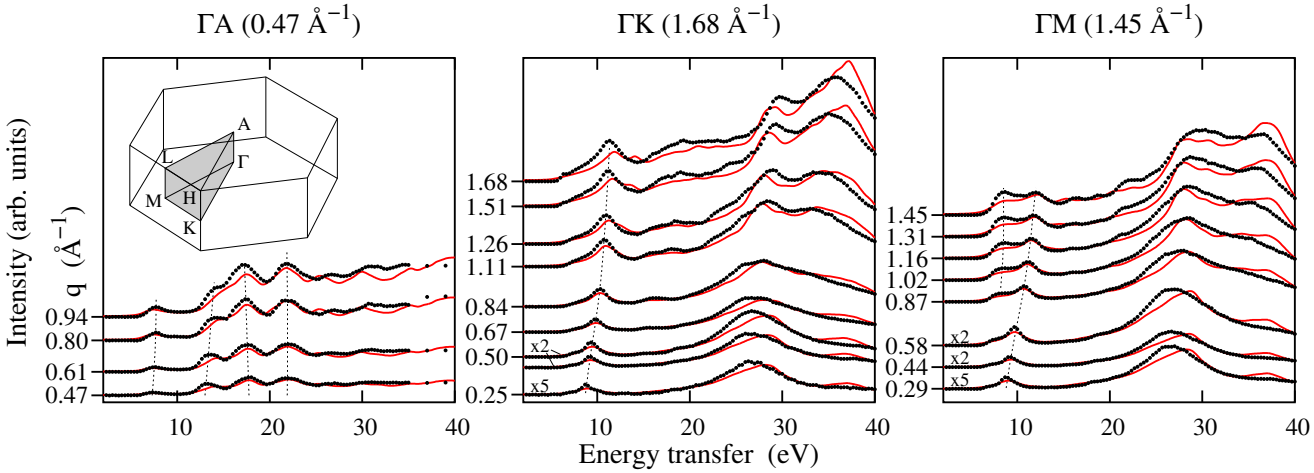

FIG. 1: (Color online) The experimental (black dots) and theoretical (red lines) NRIXS spectra for low values of momentum transfer along three crystallographic directions. The distance from Γ to the border of the 1st BZ along each direction is indicated in the titles. The q^2-weighed spectra are vertically displaced proportionally to the value of momentum transfer, which is indicated on the vertical axis. The dashed lines are guides for the eye for features discussed in the text. The inset shows the 1st BZ of *h*BN with the irreducible part shaded.

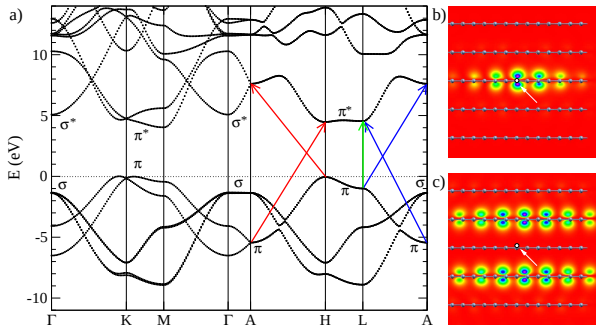

FIG. 2: (Color online) a) DFT-LDA band-structure of *h*BN. On the right the 2D projections of the electron probability density $|\Psi^{\lambda}(r_h, r_e)|^2$ for the lowest bright exciton in the optical absorption spectrum are shown with $\mathbf{q} \to 0$ b) parallel and c) perpendicular to the *h*BN planes. The hole position r_h (marked by white circle and arrow) is fixed 0.4 a.u. above a nitrogen atom. Balls and sticks indicate the atomic layers. Calculations of the excitonic wave functions have been performed using BSE.

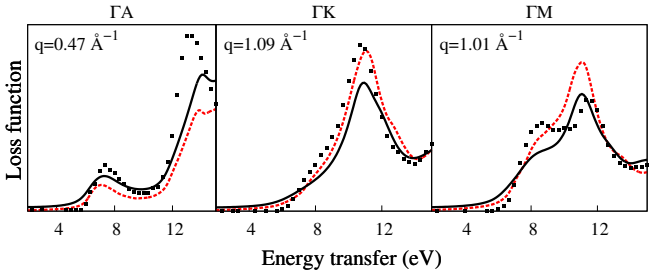

FIG. 3: (Color online) The comparison of the current RPA calculations (black solid curve) with a BSE calculation (red dashed curve) at selected momentum transfers. The RPA spectra are blueshifted as discussed in the text. Experimental data is also shown (black dots).

leads to a larger exciton binding energy for $q_{\parallel}$ than for $q_{\perp}$ and thus explains why the upshift due to the combined electron-electron and electron-hole interaction is lower for $q_{\parallel}$ than for $q_{\perp}$.

The NRIXS spectra with a larger range of momentum transfers directed along ΓK are displayed in Fig. 4. For most parts the calculated spectra agree well with the experimental ones. The prominent peak dispersing between 25-30 eV in the experimental spectra is reproduced very well by the calculations throughout the measured range of momentum transfers. At high momentum transfer (> 2 Å^{-1}) a new peak showing a small dispersion appears just above 20 eV. Its appearance and dispersion is reproduced well by the calculation. In the same momentum transfer range calculation shows a peak at around 15 eV which in the experiments appears to be less well pronounced and at a few eVs higher in energy. Around 7 eV in the high momentum transfer experimental spectra a sharp peak is observed, which is not reproduced by our RPA and BSE calculations. The origin of this peak is still to be understood.

In conclusion, we have observed an anisotropic electron-hole interaction in *h*BN. For $q_{\parallel}$ the electron and hole tend to form a strongly bound quasi-two dimensional compound while for $q_{\perp}$ the electron and hole tend to be localized on different layers and form a weakly bound three-dimensional compound. This co-existence of 2D and 3D excitons is the reason for the anisotropy of 0.7 eV in the energy shift of loss-function calculations on the

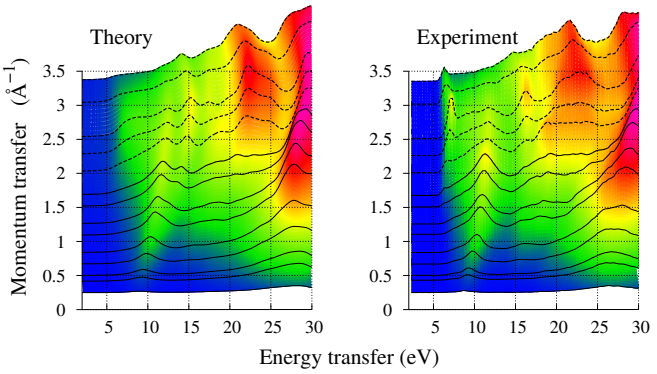

FIG. 4: (Color online) The theoretical RPA (left) and experimental (right) NRIXS spectra with the momentum transfer directed along the ΓK direction using several values of q. Spectra for which **q** lies outside the 1st BZ are drawn by dashed lines.

level of many-body perturbation theory (including excitonic effects) as compared to standard calculations on the level of the independent-particle model. Additionally, the observed anisotropic splitting of the π-plasmon and has been explained as a band structure effect arising from the anisotropic dispersion of the π-bands.

This work was supported by the Academy of Finland (1127462/110571), Spanish MEC (FIS2007-65702-C02-01), "Grupos Consolidados UPV/EHU del Gobierno Vasco" (IT-319-07), the European Community through e-I3 ETSF project (GA. 211956). JAS benefited from the CMS Network RIXS collaboration supported by the U.S. DoE (grant DE-FG02-08ER46540). LW acknowledges funding by the ANR through project ANR-09-BLAN-0421-01. AR and LW benefitted from discussions and collaborations with Prof. T. Pichler. Computing time was provided by the "Red Espanola de Supercomputación" and IDRIS (Proj. No. 091827).

[1] K. Watanabe, T. Taniguchi, and H. Kanda, Nat. Mat. **3**, 404 (2004).
[2] T. Taniguchi, K. Watanabe, and S. Koizumi, phys. stat. sol. (a) **201**, 2573 (2004).
[3] X. Blase, A. Rubio, S. G. Louie, and M. L. Cohen, Phys. Rev. B **51**, 6868 (1995).
[4] B. Arnaud, S. Lebègue, P. Rabiller, and M. Alouani, Phys. Rev. Lett. **96**, 026402 (2006).
[5] L. Wirtz, A. Marini, and A. Rubio, Phys. Rev. Lett. **96**, 126104 (2006).
[6] A. Marini, Phys. Rev. Lett. **101**, 106405 (2008).
[7] L. Wirtz, A. Marini, M. Grüning, C. Attaccalite, G. Kresse, and A. Rubio, Phys. Rev. Lett. **100**, 189701 (2008).
[8] B. Arnaud, S. Lebègue, P. Rabiller, and M. Alouani, Phys. Rev. Lett. **100**, 189702 (2008).
[9] K. Watanabe and T. Taniguchi, Phys. Rev. B **79**, 193104 (2009).
[10] P. Jaffrennou, J. Barjon, J.-S. Lauret, B. Attal-Trétout, F. Ducastelle, and A. Loiseau, J. Appl. Phys. **102**, 116102 (2008).
[11] L. Museur, E. Feldbach, and A. Kanaev, Phys. Rev. B **78**, 155204 (2008).
[12] W. A. Caliebe, J. A. Soininen, E. L. Shirley, C.-C. Kao, and K. Hämäläinen, Phys. Rev. Lett. **84**, 3907 (2000).
[13] G. G. Fuentes, E. Borowiak-Palen, T. Pichler, X. Liu, A. Graff, G. Behr, R. J. Kalenczuk, M. Knupfer, and J. Fink, Phys. Rev. B **67**, 035429 (2003).
[14] P. Abbamonte, T. Graber, J. P. Reed, S. Smadici, C. L. Yeh, A. Shukla, J. P. Rueff, and W. Ku, Proc. Nat. Acad. Sci. **105**, 12159 (2008).
[15] J. A. Soininen and E. L. Shirley, Phys. Rev. B **61**, 16423 (2000).
[16] S. Galambosi, J. A. Soininen, A. Mattila, S. Huotari, S. Manninen, G. Vankó, N. D. Zhigadlo, J. Karpinski, and K. Hämäläinen, Phys. Rev. B **71**, 060504 (2005).
[17] Y. Q. Cai, P. C. Chow, O. D. Restrepo, Y. Takano, K. Togano, H. Kito, H. Ishii, C. C. Chen, K. S. Liang, C. T. Chen, et al., Phys. Rev. Lett. **97**, 176402 (2006).
[18] Y. Kubota, K. Watanabe, O. Tsuda, and T. Taniguchi, Science **317**, 932 (2007).
[19] L. Liu, Y. P. Feng, and Z. X. Shen, Phys. Rev. B **68**, 104102 (2003).
[20] N. Ooi, A. Rairkar, L. Lindsley, and J. B. Adams, J. Phys.: Condens. Matter **18**, 97 (2006).
[21] S. Huotari, G. Vankó, F. Albergamo, C. Ponchut, H. Graafsma, C. Henriquet, R. Verbeni, and G. Monaco, J. Synchrotron Rad. **12**, 467 (2005).
[22] R. Verbeni, T. Pylkkänen, S. Huotari, L. Simonelli, G. Vankó, K. Martel, C. Henriquet, and G. Monaco, J. Synchrotron Rad. **16**, 469 (2009).
[23] K. Hämäläinen, S. Manninen, C.-C. Kao, W. Caliebe, J. B. Hastings, A. Bansil, S. Kaprzyk, and P. M. Platzman, Phys. Rev. B **54**, 5453 (1996).
[24] C. Tarrio and S. E. Schnatterly, Phys. Rev. B **40**, 7852 (1989).
[25] DFT calculations have been performed with `ABINIT`[32]. The wave-functions are expanded in plane waves with an energy cutoff of 25 Hartree. The 1s electrons are replaced by Troullier-Martins pseudopotentials. Lattice parameters $a = 2.504$ Å and $c = 6.660$ Å were used[33].
[26] S. L. Adler, Phys. Rev. **126**, 413 (1962).
[27] A. Marini, C. Hogan, M. Grüning, and D. Varsano, Comp. Phys. Comm. **180**, 1392 (2009).
[28] The matrix $\epsilon_{\mathbf{G},\mathbf{G}'}$ comprises a total of 80 **G** vectors in our calculations. The 1st BZ is sampled with a 60×60×4 k-point grid for the calculations with q parallel to the hexagonal plane and with a 30×30×12 grid for calculations with q perpendicular to it. We have included 8 occupied and 52 unoccupied bands, up to an energy of 70 eV above the valence band maximum. Calculations have been performed with `Yambo`[27].
[29] G. Onida, L. Reining, and A. Rubio, Rev. Mod. Phys. **74**, 601 (2002).

[30] L. X. Benedict and E. L. Shirley, Phys. Rev. B **59**, 5441 (1999).
[31] A k-space grid of 24×24×12, a **G**-grid of 5×5×5 and 32 unoccupied bands were used in these calculations. Finally a broadening of 0.4 eV was applied for the comparison.
[32] X. Gonze, J.-M. Beuken, R. Caracas, F. Detraux, M. Fuchs, G.-M. Rignanese, L. Sindic, M. Verstraete, G. Zerah, F. Jollet, et al., Comp. Mat. Sci. **25**, 478 (2002).
[33] V. L. Solozhenko, G. Will, and F. Elf, Solid State Commun. **96**, 1 (1995).